

ARTICLE OPEN



Exploring the capabilities of repetitive transcranial magnetic stimulation in major depressive disorder: Dynamic causal modeling of the neural network

Akira Kita ^{1,2,10}, Takuya Ishida ^{1,10}, Natsuko Kita ¹, Michiyo Tabata^{1,3}, Atsushi Tamaki¹, Shinya Uenishi^{1,4}, Kasumi Yasuda ^{1,5}, Shun Takahashi ^{1,6,7,8}, Hiroki Matsuura^{1,9}, Shinichi Yamada¹ and Sohei Kimoto ¹

© The Author(s) 2025

Repetitive transcranial magnetic stimulation (rTMS) of the left dorsal prefrontal cortex (DLPFC) has been utilized to manage treatment-resistant major depressive disorder (MDD). Understanding the biological basis of rTMS treatment in MDD is crucial for enhancing its clinical efficacy. Numerous brain regions functionally connected to the left DLPFC have been identified as a critical role in the pathophysiology of MDD, highlighting the significance of alterations in these neural circuits. We employed a dynamic causal modeling to estimate the causal relationships among depression-related regions functionally linked to the left DLPFC using a large-sample, multi-site resting-state functional magnetic resonance imaging dataset, comprising 270 healthy controls and 175 patients with MDD. We revealed aberrant causal connections from the left DLPFC, amygdala (AMY), nucleus accumbens (NAC), and thalamus (Thal) to the visual cortex (VIS) in MDD. We also found negative associations between depression severities and NAC-to-VIS connections, indicating that VIS plays an essential role in MDD. Furthermore, we identified aberrant causal connections between the ventromedial prefrontal cortex (VMPFC) and subcortical regions including, AMY, NAC, and subgenual anterior cingulate cortex (sgACC), and positive correlation between the depression severities and AMY-to-sgACC connection, suggesting the disruption in corticostriatal circuit is related to the aberrant emotional regulation in MDD. These aberrant connections may support the neural mechanisms of MDD and indicate rTMS may modulate these areas, potentially improving the disrupted function in MDD. Our study provides deeper insights into the pathophysiological mechanisms of MDD and the potential mechanisms of rTMS treatment.

Translational Psychiatry (2025)15:257; <https://doi.org/10.1038/s41398-025-03480-7>

INTRODUCTION

Major depressive disorder (MDD) is the leading cause of disease burden globally, ranking second in disability-adjusted life years according to the World Health Organization in 2020 [1, 2]. Repetitive transcranial magnetic stimulation (rTMS), which employs an excitatory pattern over the left dorsolateral prefrontal cortex (DLPFC), has been used as a non-invasive therapeutic approach in patients with treatment-resistant MDD [3] who have not responded to multiple antidepressants [4]. The canonical rTMS protocol for MDD treatment uses high-frequency stimulation (>5 Hz) over the left DLPFC [5–8]. A new rTMS protocol for MDD therapy has recently been approved by the Food and Drug Administration in the United States, namely the Stanford Intelligent Accelerated Neuromodulation Therapy (SAINT), which adopts intermittent theta burst stimulation over the left DLPFC [9] to exert excitatory effects on the left DLPFC. However, it has limited efficacy, with response rates ranging from 30–50% [10–12], primarily because its biological mechanisms are elusive. Therefore, a profound understanding of the biological foundations

underlying the rTMS treatment of MDD is essential to improve its clinical efficacy.

Previous genetic, postmortem, and neuroimaging studies have shown that MDD can be due to the dysregulation of the DLPFC circuitry. These findings include alterations in the structure, markers of synaptic neurotransmission, and connectivity abnormalities with downstream structures [13–16]. Notably, Padmanabhan et al. demonstrated, through resting-state functional magnetic resonance imaging (rs-fMRI), that brain lesion locations that induce depressive symptoms could be mapped into a connected brain circuit centered on the left DLPFC [17]. Conversely, rTMS over the left DLPFC in patients with MDD has been theorized to improve MDD by remotely modulating the distributed depression-related brain regions that are functionally connected to the left DLPFC synergetically [18–24]. Furthermore, Siddiqi et al. revealed that brain lesions inducing depressive symptoms and the stimulation sites of neuromodulation techniques for MDD converge in the same brain circuitry [25]. These findings suggest a direct causal relationship: damage to the

¹Department of Neuropsychiatry, Wakayama Medical University, Wakayama City, Wakayama Prefecture, Japan. ²Hidaka Hospital, Gobou City, Wakayama Prefecture, Japan. ³Nokami Kousei Sogo Hospital, Kimino Town, Wakayama Prefecture, Japan. ⁴Shichiyama Hospital, Kumatori Town, Osaka Prefecture, Japan. ⁵Hanwa Izumi Hospital, Izumi City, Osaka Prefecture, Japan. ⁶Department of Psychiatry, Osaka University Graduate School of Medicine, Suita City, Osaka Prefecture, Japan. ⁷Clinical Research and Education Center, Asakayama General Hospital, Sakai City, Osaka Prefecture, Japan. ⁸Graduate School of Rehabilitation Science, Osaka Metropolitan University, Habikino-City, Osaka Prefecture, Japan. ⁹Heartland Shigisan, Sango Town, Nara Prefecture, Japan. ¹⁰These authors contributed equally: Akira Kita, Takuya Ishida. ✉email: ishidafine@gmail.com

Received: 28 September 2024 Revised: 22 June 2025 Accepted: 15 July 2025

Published online: 25 July 2025

Table 1. Demographic characteristics of the participants included in the analyses.

	HCs			Patients with MDD		
	N	M/F	Age (y)	N	M/F	Age (y)
WMU	30	15/15	38.7 ± 10.0	25	9/16	43.0 ± 8.86
UTO	86	28/58	46.5 ± 15.6	58	34/24	38.3 ± 11.5
COI	61	25/36	49.6 ± 13.2	37	18/19	44.6 ± 13.0

HC healthy control, MDD major depressive disorder, WMU Wakayama Medical University, UTO University of Tokyo, COI center of innovation at Hiroshima University.

particular brain circuit triggers depression, whereas a targeted therapeutic stimulation of the same circuit alleviates depressive symptoms. This hypothesis was further substantiated by connectomics studies that demonstrated the functionally mutual connection of depression-related brain circuitry with the left DLPFC [26, 27]. These findings highlight the importance of understanding the interactions among the regions in the depression-related brain circuit connected to the left DLPFC to elucidate the disorder's pathophysiological mechanisms.

Regarding depression-related brain circuit, numerous brain regions functionally connected to the left DLPFC have been identified as critical in the pathophysiology of MDD. These include amygdala (AMY), nucleus accumbens (NAC), anterior insula (AI), subgenual anterior cingulate cortex (sgACC), and ventromedial prefrontal cortex (VMPFC). Previous studies have demonstrated that the rTMS targeting the left DLPFC modulates functional connectivity (FC) between the sgACC and other regions implicated in MDD [28, 29]. Additionally, several brain regions that psychopathologically contribute to MDD symptoms—such as the NAC, AMY, VMPFC, and insula—, functionally converge in the left DLPFC [27, 30–32]. Notably, the SAINT stimulation over the left DLPFC have been shown to improve MDD symptoms by changing the directional temporal shift between the sgACC and AI [33, 34]. In addition, the suicide preventive effects of SAINT were associated with the connection related to the insula [35]. Several studies have further revealed that these regions are components of a neural circuit broadly associated with depression. The sgACC, VMPFC and left DLPFC converge within this circuitry, integrating lesion site connectivity and neuromodulation targets [25]. Furthermore, the left DLPFC, sgACC, VMPFC, insula, NAC, and AMY form a distinct depression-specific brain circuit closely linked to emotional dysregulation in patients with MDD, as identified through connectomics methods [27]. These regions exhibit spatial correlations with the depression-related circuit delineated by Siddiqi et al. [25]. MDD results from the disruption of orchestrated functional organizations among the distributed brain regions associated with MDD; therefore, identifying the functional relationships across the brain regions in the depression-related circuit associated with the left DLPFC could provide new insights into the pathophysiological mechanisms of MDD and the biological mechanisms of rTMS treatment in patients with MDD.

Previous research has revealed aberrant FC among brain regions using traditional methods, capturing static temporal characteristics without considering the dynamic aspects of brain activity [33, 36]. However, the dynamics of whole-brain activity are crucial for regulating emotional and cognitive processes [37–42]. Dynamic causal modeling (DCM) was recently developed to investigate the dynamic patterns of brain activity by estimating the causal relationships across brain regions of interest [43]. Conventional DCM was first applied to task-based fMRI studies [43, 44]; however, a new DCM method was recently developed to evaluate the causal relationships among distributed brain areas using rs-fMRI data [30, 45–50]. Notably, several previous studies have applied this method to the rs-fMRI datasets of individuals with MDD [51–54]. However, no study has investigated the

aberrant dynamic patterns across brain areas focusing on depression-related brain circuitry in patients with MDD. Furthermore, most studies have examined aberrant FC in the brains of patients with MDD using datasets from a single site with small sample sizes [9, 36]. This limitation may have resulted in inconsistent findings across previous studies, hindering our understanding of the neural basis underlying MDD and rTMS treatment.

Here, we aimed to reveal the aberrant dynamic aspects across the regions associated with depression in patients with MDD by employing large-sample, multi-site rs-fMRI datasets comprising 270 healthy controls (HCs) and 175 patients with MDD across three imaging sites. Brain circuits functionally connected to the left DLPFC are crucial in the pathophysiological mechanisms of MDD. Consequently, we hypothesized that regions exhibiting abnormal FC with the left DLPFC might be crucial in patients with MDD. Initially, we identified areas within the whole brain that showed altered FC with the left DLPFC. We then applied DCM analysis to estimate the causal relationships among regions manifesting aberrant FC with the left DLPFC, in addition to the regions in the depression-related brain circuit such as the left DLPFC, AMY, NAC, AI, sgACC, and VMPFC. Determining the aberrant causal relationships across brain areas in the depression-related brain circuit and the regions aberrantly connected with left DLPFC could provide deeper insights into the potential mechanisms of rTMS treatment for MDD.

MATERIALS AND METHODS

Dataset and participants

In total, 445 rs-fMRI images were used from the data obtained from the Department of Psychiatry, Wakayama Medical University (WMU), and the publicly available database of the DecNef Project Brain Data Repository (<https://bicr-resource.atr.jp/srpbsoopen/>) [55]. This open dataset was collected as part of the Japanese Strategic Research Program for the Promotion of Brain Science (SRPBS) supported by the Japanese Advanced Research and Development Programs for Medical Innovation (AMED). Participants with MDD and HCs were recruited for the study from three sites: the WMU protocol, held at WMU; the University of Tokyo (UTO) protocol, held at UTO; and the Center of Innovation at Hiroshima University (COI) protocol, performed at the Hiroshima University. The latter two protocols are included in the SRPBS dataset. Overall, 270 HCs and 175 patients with MDD were recruited using the three protocols. The sample size was determined based on the previous studies performing DCM analysis [51, 52]. Notably, some participants were excluded from the analyses due to their extra head motion and misregistration of their functional image into the standard space. Therefore, 177 HCs and 120 patients with MDD were included in the analysis. Table 1 shows the demographic characteristics of all the participants included in the analyses. The demographic characteristics of all participants and MRI parameters of all sites are summarized in Supplementary Tables 1 and 2. This study was conducted in accordance with the Declaration of Helsinki and approved by the ethics committees of Wakayama Medical University (2954). Written informed consent was obtained from all participants. Figure 1 illustrates the schematics of our study flowchart.

Depressive symptoms were assessed using the 17-item version of the Hamilton Rating Scale for Depression (HAM-D) in patients with MDD at WMU. However, for patients with MDD at UTO, the Beck Depression

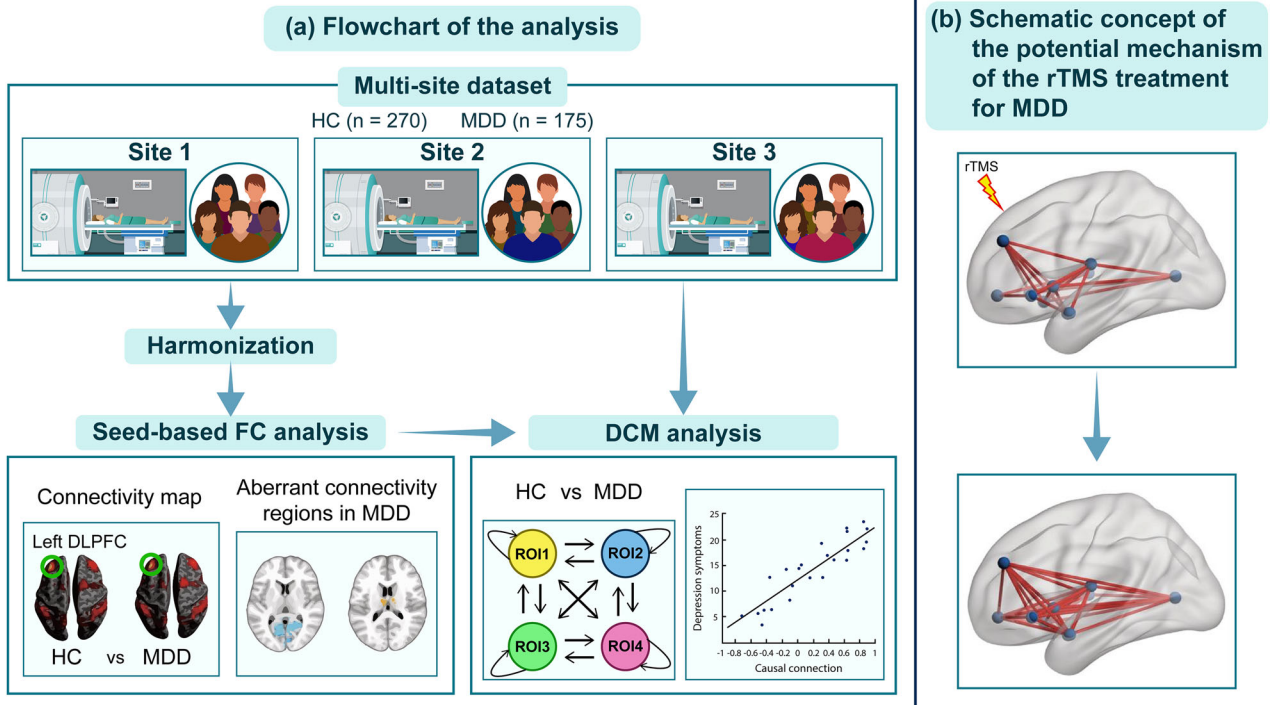


Fig. 1 Flowchart of the study protocol and schematic concept of the potential mechanism of the rTMS treatment for MDD. **a** Flowchart of the entire study protocol is shown. We employed large-sample, multi-site rs-fMRI datasets, comprising 270 HCs and 175 patients with MDD across the three imaging sites. After removing the site differences by applying ComBat harmonization, we explored the regions showing aberrant FC with the left DLPFC in patients with MDD. Furthermore, we performed DCM analysis to explore aberrant causal connections among the brain regions within the depression-related brain circuit and those aberrantly connected with left DLPFC in MDD. **b** Schematic concept of the potential mechanism of rTMS treatment for MDD is shown. We hypothesized that rTMS treatment mitigated depressive symptoms by modifying the aberrant interactions among the regions in the depression-related brain circuit and those aberrantly connected with left DLPFC in MDD. HC healthy control, MDD major depressive disorder, FC functional connectivity, DCM dynamic causal modeling, rTMS repetitive transcranial magnetic stimulation.

Table 2. The severity of depressive symptoms.

	WMU	UTO	COI
HAMD	9.44 ± 6.98 (n = 25)	-	-
BDI-II	-	20.6 ± 11.1 (n = 30)	25.3 ± 8.8 (n = 37)
CESD	-	27.9 ± 13.4 (n = 28)	-

WMU Wakayama Medical University, UTO University of Tokyo, COI center of innovation at Hiroshima University, HAMD the hamilton rating scale for depression, BDI-II the beck depression inventory revised version, CESD the center for epidemiologic studies depression scale.

Inventory revised version (BDI-II) was used to assess subjective depression symptoms for 32 patients with MDD, and the Center for Epidemiologic Studies Depression Scale (CES-D) was used to determine the depression symptoms for the 30 patients with MDD. For patients with MDD at COI, BDI-II was used to assess depressive symptoms. HAMD scores were transformed into BDI-II scores based on a study by Furukawa et al. [56]. The BDI-II and CES-D scores were then transformed into the PROMIS depression metric based on the study by Seung et al. [57].

Pre-processing of rs-fMRI data

We used SPM12 (Wellcome Department of Cognitive Neurology, <https://www.fil.ion.ucl.ac.uk/spm/>) to pre-process the MRI data. We applied slice-timing correction, and the EPI images were realigned to the first image to correct for head movements in the scanner. The corrected EPI images were co-registered to the anatomical T1 image in the native space and normalized into the Montreal Neurological Institute (MNI) space using a unified segment and Diffeomorphic

Anatomical Registration through Exponential Lie Algebra (DARTEL) in SPM12. Spatial smoothing was applied to the normalized images (2 mm isotropic voxel) with a Gaussian kernel of full-width half-maximum at 6 mm. We also normalized the segmented gray matter (GM) image to individually specify the voxels in the gray matter to extract the blood-oxygen-level-dependent (BOLD) time series. Furthermore, we normalized the segmented cerebrospinal fluid (CSF) and white matter (WM) images to extract non-neural signals of CSF and WM regions. One patient with MDD in WMU was excluded from the analysis due to the misregistration from the native space to MNI space. Patients with head motion of >2 mm were excluded from the study. Frame-to-frame head motion during the scan was evaluated using frame-wise displacement (FD) [58]. We eliminated participants whose head movement was >2 mm or >30% of the volumes having FD > 0.5 mm ("scrubbing"); therefore, 20 HCs and 16 patients with MDD in WMU, 10 HCs and 4 patients with MDD in UTO, and 63 HCs and 34 patients with MDD in COI were excluded from the analysis. Thus, 297 participants were included in the final analysis. The demographic characteristics of all participants included in the analyses are summarized in the Tables 1, 2.

Furthermore, a temporal bandpass filter (0.009–0.08 Hz) was applied for seed-based FC analysis [29, 58]. Non-neural signal sources associated with nine parameters, including the six motion parameters and average signals over the CSF, WM, and whole brain, were removed from the BOLD signal data using linear regression. For the seed-based FC analysis, we performed the scrubbing procedure by removing those volumes with FD > 0.5 mm based on a previous study [59]. FD was determined as the head motion between two consecutive volumes (the summation of absolute displacements in translation and rotation). Regarding the six motion parameters, a two-sample *t*-test showed no significant difference in head motion between the HCs and patients with MDD. Details of the results of the rs-fMRI sessions are provided in the Supplementary Results. Therefore, we did not include head-motion parameters as nuisance covariates in subsequent analyses.

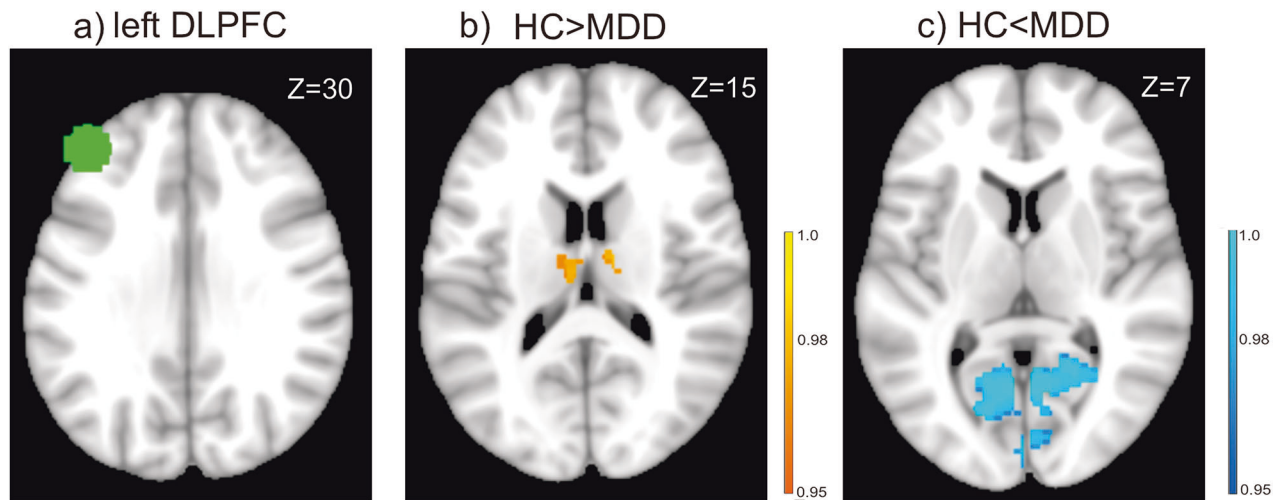


Fig. 2 Regions which showed abnormal FC with the left DLPFC in MDD. **a** The left DLPFC was used as a seed region for the FC analysis. **b** Patients with MDD had a significantly decreased FC between the bilateral Thal and left DLPFC compared with that in HCs ($p < 0.05$, corrected for multiple comparisons using the permutation method, with age and sex as nuisance covariates). **c** Patients with MDD had a significantly increased FC between the VIS and left DLPFC compared with that in HCs ($p < 0.05$, corrected for multiple comparisons using the permutation method, with age and sex as nuisance covariates). The color bar shows the $(1-p)$ values. DLPFC dorsolateral prefrontal cortex, HC healthy control, MDD major depressive disorder, FC functional connectivity, Thal thalamus, VIS visual cortex.

Region of interest specification for seed-based FC analysis and DCM

The seed mask for the left DLPFC was specified as a 10-mm radius of a spherical region of interest (ROI) centered at $[x, y, z] = [-41.25, 42.25, 29.25]$ in the MNI coordinate (Fig. 2a), which was defined by taking the average of the four MNI coordinates of the left DLPFC adopted in previous studies $[-44, 38, 34]$ and $[-38, 44, 26]$ [29], $[-42, 44, 30]$ [60], and $[-41, 43, 27]$ [61].

The ROI mask for the bilateral AMY was created using the automated anatomical labeling atlas 3 (AAL3) [62]. Based on previous studies [63–68], the ROI for the bilateral NAC included an 8-mm radius of spherical ROIs centered at $[x, y, z] = [14, 10, 0]$ and $[-14, 10, 0]$ (mm in the MNI coordinate). The ROI for the bilateral AI was specified as a 6-mm radius of spherical ROIs centered at $[x, y, z] = [-4, 25, 37]$ and $[-32, 24, -6]$ [69]. For the sgACC, the ROI mask was created a 6-mm radius of a spherical ROI centered at $[x, y, z] = [-10, 6, 16]$ based on a study by Fox et al. [29]. For the VMPFC, the ROI was specified as a 10-mm radius of a spherical ROI centered at $[x, y, z] = [0, 46, -6]$, which was defined based on previous reports on the involvement of the VMPFC in decision making [65–67].

Furthermore, we incorporated regions demonstrating abnormal FC with the left DLPFC, specifically the bilateral thalamus (Thal) and visual cortex (VIS) areas, as ROIs for subsequent DCM analyses. Using the center of gravity for the clusters identified in the FC analysis, we created the right and left Thal masks as a 6-mm radius of a spherical ROI centered at $[x, y, z] = [7.21, -12.8, 8.77]$ and $[-6.78, -14.3, 14.4]$, respectively, and a VIS mask as a 6-mm radius of a spherical ROI centered at $[x, y, z] = [-2.24, -68.9, 6.7]$. Figure 3 shows all ROIs in the DCM analysis using BrainNet Viewer (<http://www.nitrc.org/projects/bnv/>) [70].

Seed-based FC analysis and combat harmonization

We extracted the time course of all voxels included in the ROI for the left DLPFC and averaged them across all voxels in the ROI. FD was used in the subsequent scrubbing procedure [21]. FD was the head motion from one volume to the next and was calculated as the sum of the absolute values of the differentiated realignment estimates at every time point [71]. We removed volumes with $FD > 0.5$ mm to reduce spurious changes in FC due to head motion [21]. To create a whole-brain FC map, we calculated Pearson's correlation coefficients between the time course of the ROI and that of all voxels in the GM. The correlation coefficient maps were transformed into z-score maps using Fisher's r -to- z transformation.

Furthermore, we used the ComBat harmonization method to control for site differences in FC based on the adjusted general linear model harmonization method [72]. ComBat harmonization was examined using the MATLAB toolbox (<https://github.com/Jfortin1/ComBatHarmonization/>

[tree/master/Matlab](https://github.com/Jfortin1/ComBatHarmonization/)). We applied the transformed two-dimensional data with the participants' age, sex, and disease factors as covariates, along with protocol effects. The ComBat harmonization effect is shown in Supplementary Fig. 1.

After ComBat harmonization, group-level analysis for group comparison was conducted using a two-sample t -test. A threshold-free cluster enhancement (TFCE) approach was adopted with 10 000 permutations to correct for multiple comparisons, with age and sex as nuisance covariates [73]. The significance level was set at $p < 0.05$.

DCM

We employed spectral DCM implemented in SPM12 (version R7771, <http://www.fil.ion.ucl.ac.uk/spm/software/>) for the pre-processed rs-fMRI data. The DCM employs a neuronally plausible model for the observed BOLD signals and allows the estimation of causal relationships between the different nodes of the network. As described previously [30, 51], the details of DCM are provided in the Supplemental Information. Briefly, the BOLD time series of the ROIs were extracted, and non-neural signals of the WM and CSF and six head motion parameters were regressed. We used a fully connected model with bidirectional connections between any pair of ROIs for each participant. We estimated 64 free parameters because the fully connected model contained eight ROIs.

Parametric empirical bayes for group DCM

We used a standard Parametric Empirical Bayes (PEB) analysis process to conduct a group analysis and Bayes model averaging [74, 75]. The PEB took participant-specific connectivity parameters estimated from the spectral DCM to the group level, where they were modeled using a general linear model under the Bayesian hierarchical framework. Therefore, the estimated connection strengths and their uncertainties were considered from the participant to group level in the group analysis. As reported previously [30, 51], the details of these analyses are provided in the Supplementary Material.

First, we compared the causal connections across the networks between HCs and patients with MDD under the PEB framework. Age, sex, and site effects were added as nuisance covariates to the models. Furthermore, we tested the associations between causal connections and depression severity in patients with MDD under the PEB framework, with age, sex, and site effects as nuisance covariates. Depressive symptoms were assessed using the PROMIS Depression Metric [57]. We focused on connection parameters with abnormal connection values in patients with MDD. We adopted the definition of "strong evidence" by thresholding the effects at 95% posterior probability (Pp) [76]. The details of these analyses are provided in the Supplementary Material.

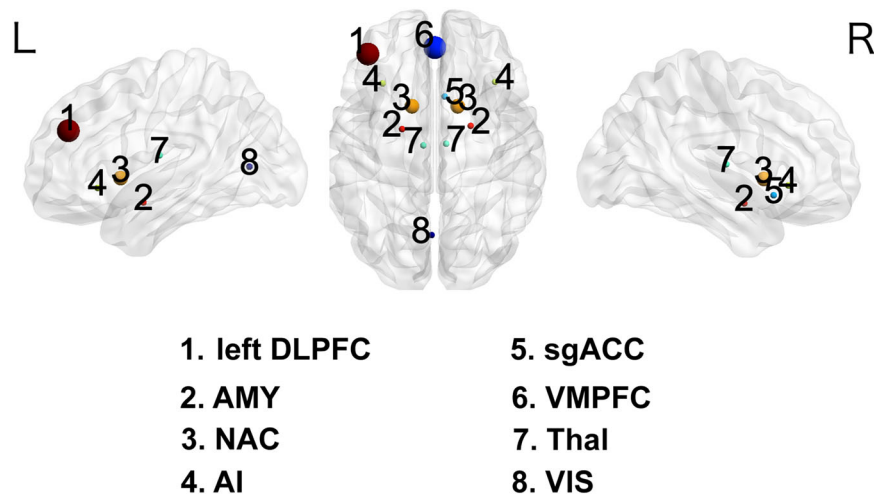


Fig. 3 Regions of interest for the DCM analysis. The ROI mask for the bilateral AMY was created using the automated anatomical labelling atlas 3 (AAL3). The ROI for the bilateral NAC comprised an 8-mm radius of spherical ROIs centered at $[x, y, z] = [14, 10, 0]$ and $[-14, 10, 0]$. The ROI for the bilateral AI was specified as a 6-mm radius of spherical ROIs centered at $[x, y, z] = [-4, 25, 37]$ and $[-32, 24, -6]$. The ROI for the sgACC was specified as a 6-mm radius of a spherical ROI centered at $[x, y, z] = [-10, 6, 16]$. The ROI for the VMPFC was specified as a 10-mm radius of a spherical ROI centered at $[x, y, z] = [0, 46, -6]$. The ROI for the bilateral Thal was created as a 6-mm radius of a spherical ROI centered at $[x, y, z] = [7.21, -12.8, 8.77]$ and $[-6.78, -14.3, 14.4]$. The ROI for the VIS was specified as a 6-mm radius of a spherical ROI centered at $[x, y, z] = [-2.24, -68.9, 6.7]$. DLPFC dorsolateral prefrontal cortex, AMY amygdala, NAC nucleus accumbens, AI anterior insula, sgACC subgenual anterior cingulate cortex, VMPFC ventromedial prefrontal cortex, Thal thalamus, VIS visual cortex, ROI region of interest, DCM dynamic causal modeling.

Table 3. Regions which showed abnormal functional connectivity with left DLPFC.

Region	Cluster Size	MNI Coordinate		
		x	y	z
HC > MDD				
Right Thalamus	82	7.21	-12.8	8.77
Left Thalamus	41	-6.78	-14.3	14.4
HC < MDD				
Visual Cortex	3701	-2.24	-68.9	6.7

DLPFC dorsolateral prefrontal cortex, HC healthy control, MDD major depressive disorder.

RESULTS

Group comparison of the seed-based FC analysis between HCs and patients with MDD

According to the study flowchart shown in Fig. 1, we initially investigated the regions displaying the aberrant FC with the left DLPFC in patients with MDD. We found that patients with MDD exhibited reduced FC between the left DLPFC seed and bilateral Thal compared with that in HCs and increased FC between the left DLPFC seed and visual areas compared with that in HCs (Fig. 2a–c and Table 3).

Group analysis of the DCM analysis between HCs and patients with MDD

Data for each group were confirmed for normal distribution using the Kolmogorov-Smirnov test and homogeneity of variances was verified using Levene's test. The mean and standard deviations of 64 parameters for HC and MDD groups are shown in Supplementary Fig. 2. We then performed DCM analysis to delineate aberrant causal connections among the brain regions in the depression-related brain circuit and those aberrantly connected with left DLPFC (Fig. 1). The ROIs included in the current DCM analysis are detailed in Fig. 3. DCM revealed that patients with MDD had increased causal connections from the AI to AMY, sgACC to NAC,

and Thal to VIS, and increased self-inhibitory connection of the AMY compared with that in HCs ($P_p > 0.95$; Fig. 4). Furthermore, MDD showed decreased causal connections from the left DLPFC to VIS, AMY to sgACC, AMY to VIS, NAC to sgACC, NAC to VIS, AI to NAC, and AI to VMPFC and decreased self-inhibitory connection of the Thal compared with that in HCs ($P_p > 0.95$; Fig. 4).

Associations between the DCM connection parameters and depression severity

Finally, we investigated the relationships between causal connections and depression severity in MDD patients (Fig. 1). The causal connection from the AMY to sgACC was positively associated with depression severity. In contrast, connections from the NAC to VIS and from the AI to VMPFC was negatively associated with depression severity in patients with MDD ($P_p > 0.95$; Fig. 5). Notably, our focus was on those connections significantly correlated with depressive severity ($P_p > 0.95$) and displaying aberrant causal connections in MDD patients compared to HCs ($P_p > 0.95$).

DISCUSSION

In this study, we used a large-sample multi-site rs-fMRI dataset of 270 HCs and 175 patients with MDD to investigate the aberrant causal connections between brain areas within the depression-related brain circuitry and brain regions aberrantly connected to the left DLPFC in MDD patients. We found that the Thal and VIS had altered FC with the left DLPFC in patients with MDD. Furthermore, we applied DCM to estimate the aberrant causal connections across brain areas within the depression-related brain circuit, including the left DLPFC, AMY, NAC, AI, sgACC, and VMPFC, as well as Thal and VIS, which were aberrantly connected to the left DLPFC in MDD. We found that patients with MDD had increased causal connections from the AI to AMY, sgACC to NAC, and Thal to VIS and increased self-inhibitory connection of the AMY compared with that in HCs. Additionally, patients with MDD showed decreased causal connections from the left DLPFC to VIS, AMY to sgACC, AMY to VIS, NAC to sgACC, NAC to VIS, AI to NAC, and AI to VMPFC and decreased self-inhibitory connection of the

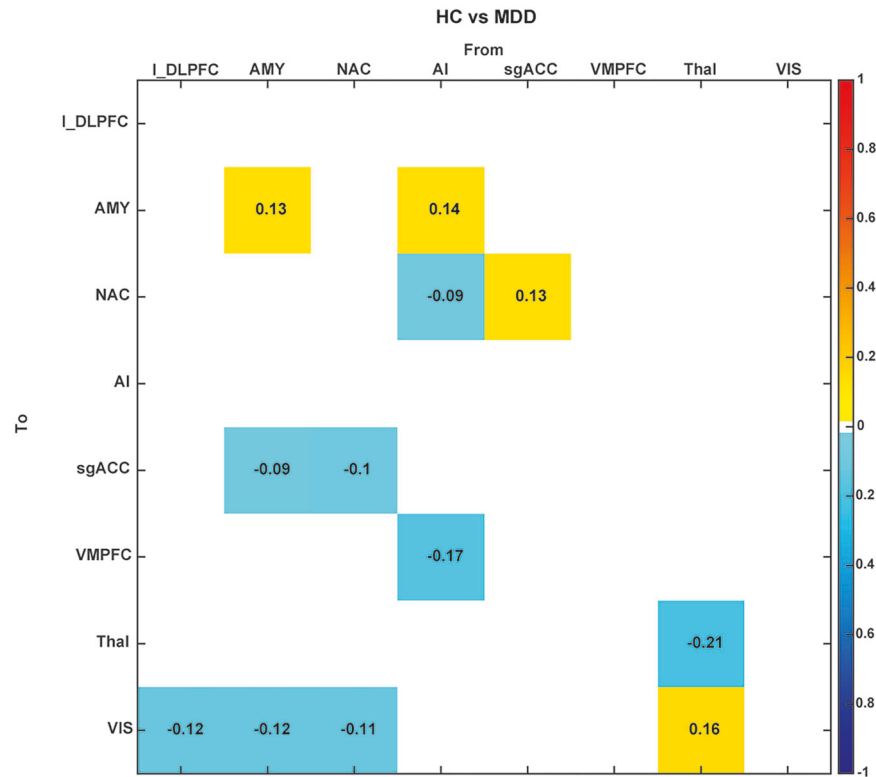


Fig. 4 Group comparison of the causal connection parameters between HCs and patients with MDD. The connection parameters whose posterior probability is more than 0.95 (strong evidence) are shown. Edges colored in yellow to red/blue indicate that the causal connection is stronger/weaker in patients with MDD than in HCs. HC healthy control, MDD major depressive disorder, DLPFC dorsolateral prefrontal cortex, AMY amygdala, NAC nucleus accumbens, AI anterior insula, sgACC subgenual anterior cingulate cortex, VMPFC ventromedial prefrontal cortex, Thal thalamus, VIS visual cortex.

Thal compared with that in HCs. Finally, we found that the causal connection from the AMY to sgACC was positively correlated with depression severity, whereas that from the NAC to VIS and from the AI to VMPFC was negatively correlated with depression severity in patients with MDD. These data suggest that aberrant causal connections across regions in the depression-related brain circuit and those aberrantly connected to left DLPFC in MDD might underpin the neural mechanisms associated with depression severity in patients with MDD.

In this study, we obtained two notable findings. Most previous studies reported that the pathophysiological mechanisms of MDD were mainly due to disruption among the higher-order brain regions [36, 48]; however, one of our main findings was that the aberrant causal connections flowed from multiple depression-related regions (left DLPFC, AMY, NAC, and Thal) to the VIS in patients with MDD, suggesting that the VIS, a primary brain region, may be essential in the mechanisms of MDD. Furthermore, we revealed aberrant causal connections between subcortical brain regions and the VMPFC. Notably, the aberrant causal connections flowed from the AI to multiple regions (AMY, NAC, and VMPFC), sgACC to NAC, and AMY to sgACC in patients with MDD, which has not been reported in previous studies. Our novel findings have not been reported previously. This may be because, first, we explored the aberrant interactions among regions in the depression-related circuitry and the regions aberrantly connected with left DLPFC in MDD using a large-sample harmonized multi-site dataset. Second, we investigated the aberrant causal connections across the ROIs using DCM, which could not be captured using FC analysis.

In addition to the novel findings of altered causal connections to the VIS in patients with MDD, we found negative correlations between depression scores and causal connections from the NAC

to VIS. Notably, some recent studies have reported abnormal functional integrity in the VIS in patients with MDD. Yang et al. [77] found that nodal degrees and efficiencies in the VIS were significantly decreased in patients with MDD. Lu et al. [78] showed that FC within the VIS was reduced in patients with MDD and that this reduced FC within the VIS was correlated with the clinical course. Other previous studies reported that the altered FC between the VIS and prefrontal cortex are crucial in the abnormal information updating processes in patients with MDD [79] and that the abnormal FC between the VIS and DLPFC could be used to predict the treatment response to electroconvulsive therapy or rTMS in patients with MDD [80]. Ding et al. [81] showed that FC between the NAC and VIS was increased in patients with MDD. Furthermore, Siddiqi et al. reported that the VIS is included in the depression-related brain circuitry [25], suggesting that damage to the occipital lobe could lead to post-stroke depression [82, 83]. These findings indicate that abnormal relationships among the VIS, subcortical regions, and prefrontal regions could greatly influence the pathophysiological mechanisms of MDD, aligning with our findings.

DCM revealed that patients with MDD had increased and decreased causal connections among certain depression-related regions, including subcortical regions and the VMPFC. Additionally, there was a reduction in self-inhibitory connections of Thal in patients with MDD compared with those in HCs. Individuals with depression show blunted responses to emotion regulation and rewarding stimuli within the corticostriatal circuit, including the AMY, NAC, AI, sgACC, VMPFC, and Thal, suggesting that disruptions in this corticostriatal circuit are fundamental in the pathophysiological mechanism of MDD [81, 84–94]. Furthermore, we found that the causal connection from the AMY to sgACC was positively correlated with depression scores. Previous studies have

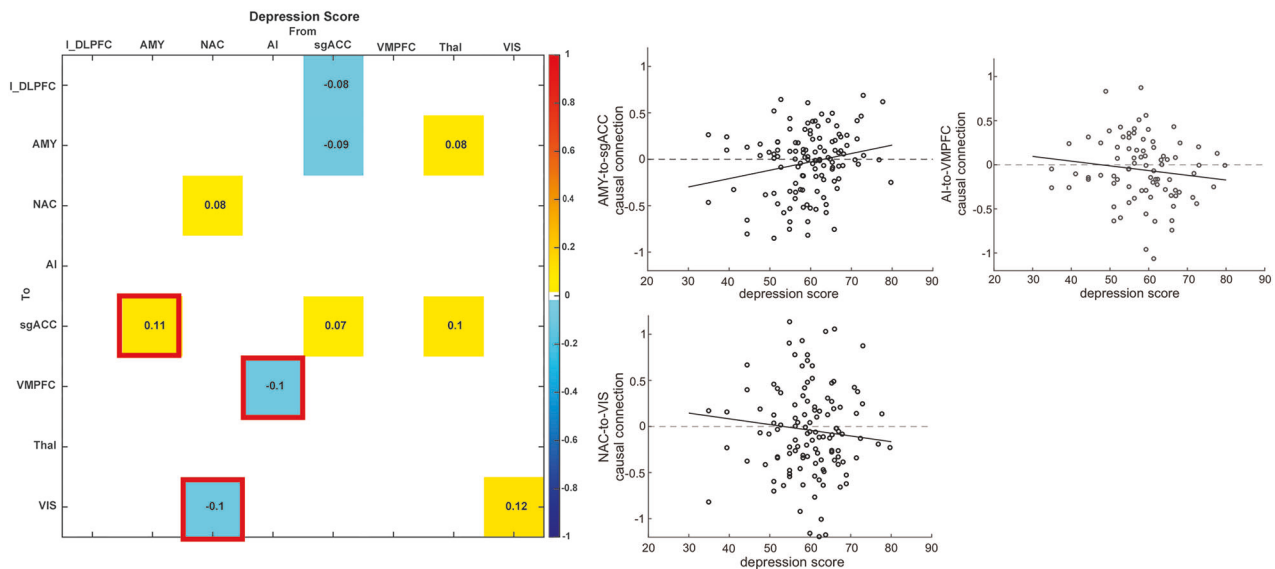


Fig. 5 Associations between the causal connection parameters and depression scores. The connections having strong evidence ($P > 0.95$) are depicted in color. The connections associated with depression scores and abnormal connections in patients with MDD were those from the AMY to sgACC, AI to VMPFC, and NAC to VIS. MDD, major depressive disorder, AMY amygdala, NAC nucleus accumbens, AI anterior insula, sgACC subgenual anterior cingulate cortex, VMPFC ventromedial prefrontal cortex, Thal thalamus, VIS visual cortex, Pp posterior probability.

shown that FC between the AMY and sgACC could be used to predict the treatment response to rTMS [95], cognitive behavioral therapy, and antidepressants [96] in patients with MDD. These studies indicate that FC between the AMY and sgACC is significant for the treatment mechanisms of MDD. However, the positive association between the causal connection from the AMY to sgACC and clinical symptoms contradicted our finding that this connection was decreased compared with that in HCs. This discrepancy suggests that normalizing the abnormal causal connection from the AMY to sgACC may not improve clinical symptoms in patients with MDD, indicating that the aberrant causal connection pattern from the AMY to sgACC in patients with MDD is qualitatively different from that in HCs. We also found that the causal connection from the AI to VMPFC was negatively correlated with depression scores, which aligns with recent findings that the FC between the VMPFC and insula decreased during emotion regulation in patients with MDD [97, 98]. Decreased causal connections from the AI to VMPFC may be important in aberrant emotion regulation in patients with MDD.

To further interpret our findings, we categorized the aberrant causal connections into two groups: (1) interconnections between regions within the depression-related circuitry and those aberrantly connected to the left DLPFC in MDD, and (2) connections within the core brain circuitry intrinsically associated with depression. From this perspective, we observed that abnormal causal flows from multiple ROIs to the VIS predominantly fell into the first category, whereas aberrant connections between subcortical regions and the VMPFC aligned with the second category. This distinction suggests that rTMS might alleviate depression by modulating not only aberrant connections within the core depression-related circuitry but also the connections between the depression-related circuit and regions that are aberrantly connected to the left DLPFC in MDD.

Finally, our results suggest the potential mechanisms underlying rTMS treatment in patients with MDD. The finding that the left DLPFC had abnormal connections with the NAC, Thal, and VIS indicates that excitatory stimulation through rTMS of the left DLPFC may remotely modulate the aberrant activity of the NAC, Thal, and VIS. This mechanism may explain the visuospatial

cognitive improvement following rTMS treatment over the left DLPFC in patients with MDD, as reported by Tsai et al. [99]. Consequently, these remote effects may extend to subcortical brain regions associated with depression, including the AMY, AI, and sgACC, potentially leading to the improvement of functional disruption among depression-related regions. Our inference regarding the potential mechanism of rTMS treatment for MDD is supported by previous studies demonstrating that neural circuits associated with MDD are functionally connected to the left DLPFC [25, 29]. Furthermore, a recent TMS/fMRI study directly demonstrated that stimulation over the left DLPFC increases activity in depression-related circuitry, including the left DLPFC, sgACC, AI, and Thal, with effects lasting at least 30 min after rTMS [100], confirming our hypothesis. However, further research is required to corroborate this hypothesis.

Limitations

First, we could not discuss the direct effects of rTMS treatment in patients with MDD because most participants with MDD in our study did not receive rTMS treatment. Second, we had limited medication data for the datasets and did not test for non-medicated patients; therefore, we could not eliminate the effect of medications on the results. Third, we did not have any data on illness duration or clinical states, such as acute or remitted, and we did not estimate their effects on the causal connections among the brain regions. Fourth, rTMS is predominantly administered to individuals with treatment-resistant depression, defined as those who have not responded to at least one antidepressant. Therefore, there may be differences between the MDD sample in this study and the typical treatment-resistant population.

Conclusion

DCM revealed aberrant causal connections among the regions in the depression-related circuits and those aberrantly connected with left DLPFC in MDD, including the left DLPFC, AMY, NAC, AI, sgACC, VMPFC, Thal, and VIS, and their associations with depressive symptoms. Our findings provide deeper insight into the pathophysiological mechanisms of MDD and elucidate the potential mechanisms of rTMS treatment in patients with MDD.

DATA AVAILABILITY

The source code and scripts that support study findings are available from the corresponding author, TI, upon reasonable request.

REFERENCES

- Wittchen HU, Jacobi F, Rehm J, Gustavsson A, Svensson M, Jönsson B, et al. The size and burden of mental disorders and other disorders of the brain in Europe 2010. *Eur Neuropsychopharmacol.* 2011;21:655–79.
- Moussavi S, Chatterji S, Verdes E, Tandon A, Patel V, Ustun B. Depression, chronic diseases, and decrements in health: results from the World Health Surveys. *Lancet.* 2007;370:851–8.
- Blumberger DM, Vila-Rodriguez F, Thorpe KE, Feffer K, Noda Y, Giacobbe P, et al. Effectiveness of theta burst versus high-frequency repetitive transcranial magnetic stimulation in patients with depression (THREE-D): a Randomised Non-Inferiority Trial. *Lancet.* 2018;391:1683–92.
- Rush AJ, Warden D, Wisniewski SR, Fava M, Trivedi MH, Gaynes BN, et al. STAR*D. *CNS Drugs.* 2009;23:627–47.
- O'Reardon JP, Solvason HB, Janicak PG, Sampson S, Isenberg KE, Nahas Z, et al. Efficacy and safety of transcranial magnetic stimulation in the acute treatment of major depression: a multisite Randomized Controlled Trial. *Biol Psychiatry.* 2007;62:1208–16.
- Avery DH, Holtzheimer PE, Fawaz W, Russo J, Neumaier J, Dunner DL, et al. A controlled study of repetitive transcranial magnetic stimulation in medication-resistant major depression. *Biol Psychiatry.* 2006;59:187–94.
- Gaynes BN, Lloyd SW, Lux L, Gartlehner G, Hansen RA, Brode S, et al. Repetitive transcranial magnetic stimulation for treatment-resistant depression: a systematic review and meta-analysis. *J Clin Psychiatry.* 2014;75:477–89.
- Berlim MT, van den Eynde F, Tovar-Perdomo S, Daskalakis ZJ. Response, remission and drop-out rates following high-frequency repetitive transcranial magnetic stimulation (rTMS) for treating major depression: a systematic review and meta-analysis of randomized, double-blind and Sham-Controlled Trials. *Psychol Med.* 2014;44:225–39.
- Cole EJ, Stimpson KH, Bentzley BS, Gulser M, Cherian K, Tischler C, et al. Stanford accelerated intelligent neuromodulation therapy for treatment-resistant depression. *Am J Psychiatry.* 2020;177:716–26.
- Fitzgerald PB. An update on the clinical use of repetitive transcranial magnetic stimulation in the treatment of depression. *J Affect Disord.* 2020;276:90–103.
- Miron J-P, Jodoin VD, Lespérance P, Blumberger DM. Repetitive transcranial magnetic stimulation for major depressive disorder: basic principles and future directions. *Ther Adv Psychopharmacol.* 2021;11:204512532110426.
- Imazu S, Ikeda S, Toi Y, Sano S, Kanazawa T, Shinosaki K, et al. Real-world outcome of rTMS treatment for depression within the Japanese public health insurance system: registry data from Kansai TMS network. *Asian J Psychiatr.* 2024;97:104082.
- Wu J, Li Y, Huang Y, Liu L, Zhang H, Nagy C, et al. Integrating spatial and single-nucleus transcriptomic data elucidates microglial-specific responses in female cynomolgus macaques with depressive-like behaviors. *Nat Neurosci.* 2023;26:1352–64.
- Nagy C, Maitra M, Tanti A, Suderman M, Théroneux JF, Davoli MA, et al. Single-nucleus transcriptomics of the prefrontal cortex in major depressive disorder implicates oligodendrocyte precursor cells and excitatory neurons. *Nat Neurosci.* 2020;23:771–81.
- Brody AL, Saxena S, Mandelkern MA, Fairbanks LA, Ho ML, Baxter LR. Brain metabolic changes associated with symptom factor improvement in major depressive disorder. *Biol Psychiatry.* 2001;50:171–8.
- Gold PW. The organization of the stress system and its dysregulation in depressive illness. *Mol Psychiatry.* 2015;20:32–47.
- Padmanabhan JL, Cooke D, Joutsa J, Siddiqi SH, Ferguson M, Darby RR, et al. A human depression circuit derived from focal brain lesions. *Biol Psychiatry.* 2019;86:749–58.
- Eldaief MC, Halko MA, Buckner RL, Pascual-Leone A. Transcranial magnetic stimulation modulates the brain's intrinsic activity in a frequency-dependent manner. *Proc Natl Acad Sci USA.* 2011;108:21229–34.
- van der Werf YD, Sanz-Arigita EJ, Menning S, van den Heuvel OA. Modulating spontaneous brain activity using repetitive transcranial magnetic stimulation. *BMC Neurosci.* 2010;11:145.
- Vercammen A, Knegtering H, Liemburg EJ, Boer JA, den, Aleman A. Functional connectivity of the temporo-parietal region in schizophrenia: effects of rTMS treatment of auditory hallucinations. *J Psychiatr Res.* 2010;44:725–31.
- Shafi MM, Westover MB, Fox MD, Pascual-Leone A. Exploration and modulation of brain network interactions with noninvasive brain stimulation in combination with neuroimaging. *Eur J Neurosci.* 2012;35:805–25.
- Reithler J, Peters JC, Sack AT. Multimodal transcranial magnetic stimulation: Using concurrent neuroimaging to reveal the neural network dynamics of noninvasive brain stimulation. *Prog Neurobiol.* 2011;94:149–65.
- Bestmann S, Baudewig J, Siebner HR, Rothwell JC, Frahm J. Subthreshold high-frequency TMS of human primary motor cortex modulates interconnected frontal motor areas as detected by interleaved fMRI-TMS. *Neuroimage.* 2003;20:1685–96.
- Chouinard PA, Van Der Werf YD, Leonard G, Paus T. Modulating neural networks with transcranial magnetic stimulation applied over the dorsal premotor and primary motor cortices. *J Neurophysiol.* 2003;90:1071–83.
- Siddiqi SH, Schaper FLWVJ, Horn A, Hsu J, Padmanabhan JL, Brodtmann A, et al. Brain stimulation and brain lesions converge on common causal circuits in neuropsychiatric disease. *Nat Hum Behav.* 2021;5:1707–16.
- Eldaief MC, McMains S, Izquierdo-Garcia D, Daneshmand M, Nummenmaa A, Braga RM. Network-specific metabolic and haemodynamic effects elicited by non-invasive brain stimulation. *Nat Ment Health.* 2023;1:346–60.
- Cash RFH, Müller VI, Fitzgerald PB, Eickhoff SB, Zalesky A. Altered brain activity in unipolar depression unveiled using connectomics. *Nat Ment Health.* 2023;1:174–85.
- Avissar M, Powell F, Ilieva I, Respingo M, Gunning FM, Liston C, et al. Functional connectivity of the left DLPFC to striatum predicts treatment response of depression to TMS. *Brain Stimul.* 2017;10:919–25.
- Fox MD, Buckner RL, White MP, Greicius MD, Pascual-Leone A. Efficacy of transcranial magnetic stimulation targets for depression is related to intrinsic functional connectivity with the subgenual cingulate. *Biol Psychiatry.* 2012;72:595–603.
- Ishida T, Dierks T, Strik W, Morishima Y. Converging resting state networks unravels potential remote effects of transcranial magnetic stimulation for major depression. *Front Psychiatry.* 2020;11:836.
- Russo SJ, Nestler EJ. The brain reward circuitry in mood disorders. *Nat Rev Neurosci.* 2013;14:609–25.
- Nestler EJ, Carlezon WA. The mesolimbic dopamine reward circuit in depression. *Biol Psychiatry.* 2006;59:1151–9.
- Manoliu A, Meng C, Brandl F, Doll A, Tahmasian M, Scherr M, et al. Insular dysfunction within the salience network is associated with severity of symptoms and aberrant inter-network connectivity in major depressive disorder. *Front Hum Neurosci.* 2014;7:930.
- Mitra A, Raichle ME, Geoly AD, Kratter IH, Williams NR. Targeted neurostimulation reverses a spatiotemporal biomarker of treatment-resistant depression. *Proc Natl Acad Sci.* 2023;120:e2218958120.
- Li B, Zhao N, Tang N, Friston KJ, Zhai W, Wu D, et al. Targeting suicidal ideation in major depressive disorder with MRI-navigated Stanford accelerated intelligent neuromodulation therapy. *Transl Psychiatry.* 2024;14:21.
- Kaiser RH, Andrews-Hanna JR, Wager TD, Pizzagalli DA. Large-scale network dysfunction in major depressive disorder: a meta-analysis of resting-state functional connectivity. *JAMA Psychiatry.* 2015;72:603–11.
- Mitra A, Snyder AZ, Hacker CD, Pahwa M, Tagliazucchi E, Laufs H, et al. Human cortical-hippocampal dialogue in wake and slow-wave sleep. *Proc Natl Acad Sci USA.* 2016;113:E6868–E6876.
- Mitra A, Snyder AZ, Tagliazucchi E, Laufs H, Raichle ME. Propagated infra-slow intrinsic brain activity reorganizes across wake and slow wave sleep. *Elife.* 2015;4:e10781.
- Razi A, Seghier ML, Zhou Y, McColgan P, Zeidman P, Park HJ, et al. Large-scale DCMs for resting-state fMRI. *Network. Neuroscience.* 2017;1:222–41.
- Watanabe T, Rees G. Brain network dynamics in high-functioning individuals with autism. *Nat Commun.* 2017;8:16048.
- Braun U, Schäfer A, Walter H, Erk S, Romanczuk-Seiferth N, Haddad L, et al. Dynamic reconfiguration of frontal brain networks during executive cognition in humans. *Proc Natl Acad Sci USA.* 2015;112:11678–83.
- Kucyi A, Hove MJ, Esterman M, Matthew Hutchison R, Valera EM. Dynamic brain network correlates of spontaneous fluctuations in attention. *Cereb Cortex.* 2017;27:1831–40.
- Friston KJ, Harrison L, Penny W. Dynamic causal modelling. *Neuroimage.* 2003;19:1273–302.
- Stephan KE, Penny WD, Marshall JC, Fink GR, Friston KJ. Investigating the functional role of callosal connections with dynamic causal models. *Ann N Y Acad Sci.* 2005;1064:16–36.
- Bastos-Leite AJ, Ridgway GR, Silveira C, Norton A, Reis S, Friston KJ. Dysconnectivity within the default mode in first-episode schizophrenia: a stochastic dynamic causal modeling study with functional magnetic resonance imaging. *Schizophr Bull.* 2015;41:144–53.
- Chahine G, Richter A, Wolter S, Goya-Maldonado R, Gruber O. Disruptions in the left frontoparietal network underlie resting state endophenotypic markers in Schizophrenia. *Hum Brain Mapp.* 2017;38:1741–50.

47. Di X, Biswal BB. Identifying the default mode network structure using dynamic causal modeling on resting-state functional magnetic resonance imaging. *Neuroimage*. 2014;86:53–9.
48. Li L, Li B, Bai Y, Liu W, Wang H, Leung HC, et al. Abnormal resting state effective connectivity within the default mode network in major depressive disorder: a spectral dynamic causal modeling study. *Brain Behav*. 2017;7:e00732.
49. Razi A, Kahan J, Rees G, Friston KJ. Construct validation of a DCM for resting state fMRI. *Neuroimage*. 2015;106:1–14.
50. Xu J, Yin X, Ge H, Han Y, Pang Z, Liu B, et al. Heritability of the effective connectivity in the resting-state default mode network. *Cereb Cortex*. 2017;27:5626–34.
51. Ishida T, Nakamura Y, Tanaka SC, Mitsuyama Y, Yokoyama S, Shinzato H, et al. Aberrant large-scale network interactions across psychiatric disorders revealed by large-sample multi-site resting-state functional magnetic resonance imaging datasets. *Schizophr Bull*. 2023;49:933–43. <https://doi.org/10.1093/schbul/sbad022>
52. Nakamura Y, Ishida T, Tanaka SC, Mitsuyama Y, Yokoyama S, Shinzato H, et al. Distinctive alterations in the mesocorticolimbic circuits in various psychiatric disorders PCN psychiatry and clinical neurosciences. *Psychiatry Clin Neurosci*. 2023;77:345–54.
53. Li G, Liu Y, Zheng Y, Li D, Liang X, Chen Y, et al. Large-scale dynamic causal modeling of major depressive disorder based on resting-state functional magnetic resonance imaging. *Hum Brain Mapp*. 2020;41:865–81.
54. Ray D, Bezmaternykh D, Mel'nikov M, Friston KJ, Das M. Altered effective connectivity in sensorimotor cortices is a signature of severity and clinical course in depression. *Proc Natl Acad Sci*. 2021;118:e2105730118.
55. Tanaka SC, Yamashita A, Yahata N, Itahashi T, Lisi G, Yamada T, et al. A multi-site, multi-disorder resting-state magnetic resonance image database. *Sci Data*. 2021;8:227.
56. Furukawa TA, Reijnders M, Kishimoto S, Sakata M, DeRubeis RJ, Dimidjian S, et al. Translating the BDI and BDI-II into the HAMD and vice versa with equipercentile linking. *Epidemiol Psychiatr Sci*. 2020;29:e24.
57. Choi SW, Schalet B, Cook KF, Cella D. Establishing a common metric for depressive symptoms: linking the BDI-II, CES-D, and PHQ-9 to PROMIS depression. *Psychol Assess*. 2014;26:513–27.
58. Lowe MJ, Mock BJ, Sorenson JA. Functional connectivity in single and multislice echoplanar imaging using resting-state fluctuations. *Neuroimage*. 1998;7:119–32.
59. Power JD, Barnes KA, Snyder AZ, Schlaggar BL, Petersen SE. Spurious but systematic correlations in functional connectivity MRI networks arise from subject motion. *Neuroimage*. 2012;59:2142–54.
60. Weigand A, Horn A, Caballero R, Cooke D, Stern AP, Taylor SF, et al. Prospective validation that subgenual connectivity predicts antidepressant efficacy of transcranial magnetic stimulation sites. *Biol Psychiatry*. 2018;84:28–37.
61. Cash RH, Zalesky A, Thomson RH, Tian Y, Cocchi L, Fitzgerald PB. Subgenual functional connectivity predicts antidepressant treatment response to transcranial magnetic stimulation: independent validation and evaluation of personalization. *Biol Psychiatry*. 2019;86:e5–e7.
62. Rolls ET, Huang CC, Lin CP, Feng J, Joliot M. Automated anatomical labelling atlas 3. *Neuroimage*. 2020;206:116189.
63. Pizzagalli DA, Holmes AJ, Dillon DG, Goetz EL, Birk JL, Bogdan R, et al. Reduced caudate and nucleus accumbens response to rewards in unmedicated individuals with major depressive disorder. *Am J Psychiatry*. 2009;166:702–10.
64. Monk CS, Klein RG, Telzer EH, Elizabeth Schroth BA, Salvatore Mannuzza B, Moulton JL III, et al. Article amygdala and nucleus accumbens activation to emotional facial expressions in children and adolescents at risk for major depression. *Am J Psychiatry*. 2008;165:90–8.
65. Keedwell PA, Andrew C, Williams SCR, Brammer MJ, Phillips ML. A double dissociation of ventromedial prefrontal cortical responses to sad and happy stimuli in depressed and healthy individuals. *Biol Psychiatry*. 2005;58:495–503.
66. Greicius MD, Krasnow B, Reiss AL, Menon V, Raichle ME. Functional connectivity in the resting brain: a network analysis of the default mode hypothesis. *Proc Natl Acad Sci USA*. 2003;100:253–8.
67. Knutson B, Bhanji JP, Cooney RE, Atlas LY, Gotlib IH. Neural responses to monetary incentives in major depression. *Biol Psychiatry*. 2008;63:686–92.
68. Zhang WN, Chang SH, Guo LY, Zhang KL, Wang J. The neural correlates of reward-related processing in major depressive disorder: a meta-analysis of functional magnetic resonance imaging studies. *J Affect Disord*. 2013;151:531–9.
69. Sridharan D, Levitin DJ, Menon V. A critical role for the right fronto-insular cortex in switching between central-executive and default-mode networks. *Proc Natl Acad Sci USA*. 2008;105:12569–74.
70. Xia M, Wang J, He Y. BrainNet viewer: a network visualization tool for human brain connectomics. *PLoS One*. 2013;8:e68910.
71. Power JD, Mitra A, Laumann TO, Snyder AZ, Schlaggar BL, Petersen SE. Methods to detect, characterize, and remove motion artifact in resting state fMRI. *Neuroimage*. 2014;84:320–41.
72. Johnson WE, Li C, Rabinovic A. Adjusting batch effects in microarray expression data using empirical Bayes methods. *Biostatistics*. 2007;8:118–27.
73. Smith SM, Nichols TE. Threshold-free cluster enhancement: addressing problems of smoothing, threshold dependence and localisation in cluster inference. *Neuroimage*. 2009;44:83–98.
74. Zeidman P, Jafarian A, Seghier ML, Litvak V, Cagnan H, Price CJ, et al. A guide to group effective connectivity analysis, part 2: second level analysis with PEB. *Neuroimage*. 2019;200:12–25.
75. Friston KJ, Litvak V, Oswal A, Razi A, Stephan KE, Van Wijk BCM, et al. Bayesian model reduction and empirical Bayes for group (DCM) studies. *Neuroimage*. 2016;128:413–31.
76. Kass RE, Raftery AE. Bayes factors. *J Am Stat Assoc*. 1995;90:773–95.
77. Yang H, Chen X, Chen ZB, Li L, Li XY, Castellanos FX, et al. Disrupted intrinsic functional brain topology in patients with major depressive disorder. *Mol Psychiatry*. 2021;26:7363–71.
78. Lu F, Cui Q, Huang X, Li L, Duan X, Chen H, et al. Anomalous intrinsic connectivity within and between visual and auditory networks in major depressive disorder. *Prog Neuropsychopharmacol Biol Psychiatry*. 2020;100:109889.
79. Le TM, Borghi JA, Kujawa AJ, Klein DN, Leung HC. Alterations in visual cortical activation and connectivity with prefrontal cortex during working memory updating in major depressive disorder. *Neuroimage Clin*. 2017;14:43–53.
80. Moreno-Ortega M, Prudic J, Rowny S, Patel GH, Kangarlu A, Lee S, et al. Resting state functional connectivity predictors of treatment response to electroconvulsive therapy in depression. *Sci Rep*. 2019;9:5071.
81. Ding YD, Chen X, Chen ZB, Li L, Li XY, Castellanos FX, et al. Reduced nucleus accumbens functional connectivity in reward network and default mode network in patients with recurrent major depressive disorder. *Transl Psychiatry*. 2022;12:236.
82. Sutoko S, Atsumori H, Obata A, Funane T, Kandori A, Shimonaga K, et al. Lesions in the right Rolandic operculum are associated with self-rating affective and apathetic depressive symptoms for post-stroke patients. *Sci Rep*. 2020;10:20264.
83. Santos M, Kövari E, Gold G, Bozikas VP, Hof PR, Bouras C, et al. The neuroanatomical model of post-stroke depression: towards a change of focus? *J Neurol Sci*. 2009;283:158–62.
84. Rappaport BI, Kandala S, Luby JL, Barch DM. Brain reward system dysfunction in adolescence: current, cumulative, and developmental periods of depression. *Am J Psychiatry*. 2020;177:754–63.
85. Dichter GS, Kozink RV, McClernon FJ, Smoski MJ. Remitted major depression is characterized by reward network hyperactivation during reward anticipation and hypoactivation during reward outcomes. *J Affect Disord*. 2012;136:1126–34.
86. Hiser J, Koenigs M. The multifaceted role of the ventromedial prefrontal cortex in emotion, decision making, social cognition, and psychopathology. *Biol Psychiatry*. 2018;83:638–47.
87. Stringaris A, Belil PVR, Artiges E, Lemaître H, Gollier-Briant F, Wolke S, et al. The brain's response to reward anticipation and depression in adolescence: dimensionality, specificity, and longitudinal predictions in a community-based sample. *Am J Psychiatry*. 2015;172:1215–23.
88. Keren H, O'Callaghan G, Vidal-Ribas P, Buzzell GA, Brotman MA, Leibenluft E, et al. Reward processing in depression: a conceptual and meta-analytic review across fMRI and EEG studies. *Am J Psychiatry*. 2018;175:1111–20.
89. Zhang Y, Shao J, Wang X, Chen Z, Liu H, Pei C, et al. Functional impairment-based segmentation of anterior cingulate cortex in depression and its relationship with treatment effects. *Hum Brain Mapp*. 2021;42:4035–47.
90. Bewernick BH, Hurlmann R, Matusch A, Kayser S, Grubert C, Hadrysiewicz B, et al. Nucleus accumbens deep brain stimulation decreases ratings of depression and anxiety in treatment-resistant depression. *Biol Psychiatry*. 2010;67:110–6.
91. Schlaepfer TE, Cohen MX, Frick C, Kosel M, Brodesser D, Axmacher N, et al. Deep brain stimulation to reward circuitry alleviates anhedonia in refractory major depression. *Neuropsychopharmacology*. 2008;33:368–77.
92. Malone DA, Dougherty DD, Rezai AR, Carpenter LL, Friehs GM, Eskandar EN, et al. Deep brain stimulation of the ventral capsule/ventral striatum for treatment-resistant depression. *Biol Psychiatry*. 2009;65:267–75.
93. Hitti FL, Cristancho MA, Yang AI, O'Reardon JP, Bhati MT, Baltuch GH. Deep brain stimulation of the ventral capsule/ventral striatum for treatment-resistant depression: a decade of clinical follow-up. *J Clin Psychiatry*. 2021;82:21m13973.
94. Du L, Liu H, Du W, Chao F, Zhang L, Wang K, et al. Stimulated left DLPFC-nucleus accumbens functional connectivity predicts the anti-depression and anti-anxiety effects of rTMS for depression. *Transl Psychiatry*. 2017;7:3.
95. Salomons TV, Dunlop K, Kennedy SH, Flint A, Geraci J, Giacobbe P, et al. Resting-state cortico-thalamic-striatal connectivity predicts response to dorsomedial

- prefrontal rTMS in major depressive disorder. *Neuropsychopharmacology*. 2014;39:488–98.
96. Jamieson AJ, Harrison BJ, Razi A, Davey CG. Rostral anterior cingulate network effective connectivity in depressed adolescents and associations with treatment response in a Randomized Controlled Trial. *Neuropsychopharmacology*. 2022;47:1240–8.
 97. Young CB, Chen T, Nusslock R, Keller J, Schatzberg AF, Menon V. Anhedonia and general distress show dissociable ventromedial prefrontal cortex connectivity in major depressive disorder. *Transl Psychiatry*. 2016;6:e810.
 98. Li L, Li R, Shen F, Wang X, Zou T, Deng C, et al. Negative bias effects during audiovisual emotional processing in major depression disorder. *Hum Brain Mapp*. 2022;43:1449–62.
 99. Tsai PY, Chen YC, Wang JY, Chung KH, Lai CH. Effect of repetitive transcranial magnetic stimulation on depression and cognition in individuals with traumatic brain injury: a systematic review and meta-analysis. *Sci Rep*. 2021;11:16940.
 100. Tik M, Woletz M, Schuler AL, Vasileiadi M, Cash RFH, Zalesky A, et al. Acute TMS/fMRI response explains offline TMS network effects – an interleaved TMS-fMRI study. *Neuroimage*. 2023;267:119833.

ACKNOWLEDGEMENTS

Our research was supported by JSPS KAKENHI Grant Number 18K07570, 20K16675, 21K07484, 23K06992 and 24K18744, the Naito Foundation, and the Osaka Medical Research Foundation for Intractable Diseases.

AUTHOR CONTRIBUTIONS

AK, TI, SK contributed to the conception, design of the study. NK, MT, AT, SU, KY contributed to data acquisition of the study. AK and TI performed data analysis. AK, TI, SK contributed to the interpretation of the data. TS, HM, SY, and SK contributed to drafting the article or revising it critically for important intellectual content. All authors gave final approval of the version to be published.

COMPETING INTERESTS

The authors declare no competing interests.

ADDITIONAL INFORMATION

Supplementary information The online version contains supplementary material available at <https://doi.org/10.1038/s41398-025-03480-7>.

Correspondence and requests for materials should be addressed to Takuya Ishida.

Reprints and permission information is available at <http://www.nature.com/reprints>

Publisher's note Springer Nature remains neutral with regard to jurisdictional claims in published maps and institutional affiliations.



Open Access This article is licensed under a Creative Commons Attribution-NonCommercial-NoDerivatives 4.0 International License, which permits any non-commercial use, sharing, distribution and reproduction in any medium or format, as long as you give appropriate credit to the original author(s) and the source, provide a link to the Creative Commons licence, and indicate if you modified the licensed material. You do not have permission under this licence to share adapted material derived from this article or parts of it. The images or other third party material in this article are included in the article's Creative Commons licence, unless indicated otherwise in a credit line to the material. If material is not included in the article's Creative Commons licence and your intended use is not permitted by statutory regulation or exceeds the permitted use, you will need to obtain permission directly from the copyright holder. To view a copy of this licence, visit <http://creativecommons.org/licenses/by-nc-nd/4.0/>.

© The Author(s) 2025